

# Warm Dark Matter: The End is Nigh

Aurel Schneider<sup>1\*</sup>, Donnino Anderhalden<sup>2</sup>, Andrea V. Macciò<sup>3</sup>, and Jürg Diemand<sup>2</sup>

<sup>1</sup>*Department of Physics and Astronomy, University of Sussex, Brighton, BN1 9QH, UK*

<sup>2</sup>*Institute for Theoretical Physics, University of Zurich, 8057 Zurich, Switzerland*

<sup>3</sup>*Max Planck Institut für Astronomie, Königstuhl 17, D-69117 Heidelberg, Germany*

(Dated: June 19, 2017)

Over the last decade warm dark matter (WDM) has been repeatedly proposed as an alternative scenario to the standard cold dark matter (CDM) one, potentially resolving several disagreements between the CDM model and observations on small scales. Here we reconsider the most important CDM small scale discrepancies in the light of recent observational constraints on WDM. As a result, we find that a conventional thermal (or thermal-like) WDM cosmology with a particle mass in agreement with Lyman- $\alpha$  is nearly indistinguishable from CDM on the relevant scales and therefore fails to alleviate any of the small scale problems. The reason for this failure is that the power spectrum of conventional WDM falls off too rapidly. To maintain WDM as a significantly different alternative to CDM, more evolved production mechanisms leading to multiple dark matter components and a gradually decreasing small scale power spectrum have to be considered.

*Introduction.*— While the standard model of cosmology,  $\Lambda$ CDM, is an indisputable success on large scales, it has several potential problems on smaller scales. Examples are the overabundance of dwarf galaxies in the Milky-Way galaxy [1, 2], the local group [3], and local voids [4], or an excess of dark matter in the centres of dwarf galaxies [5]. Whether these discrepancies are a result of our poor understanding of galaxy formation or if they are a hint for an alternative form of dark matter is currently under debate [6].

One of the most popular alternative dark matter scenarios, which seems to naturally solve many of the small scale disagreements while being indistinguishable from CDM on larger scales, is the warm dark matter (WDM) paradigm, where the power spectrum is characterised by steep cutoff at the dwarf galaxy scales [7]. Due to the lack of small scale power, WDM structure formation is suppressed, resulting in a reduced dwarf galaxy abundance and shallower inner profiles, which are in better agreement with observations [8–10].

The most popular candidate for WDM is the sterile neutrino, which naturally arises from a minimal extension of the neutrino sector within the standard model, motivated by the recently observed neutrino oscillation [11]. In the early universe, sterile neutrinos can be produced by resonant oscillation of active neutrinos [12], a production mechanism that evades observational constraints as long as a significant lepton asymmetry is assumed [13]. Resonantly produced sterile neutrinos are not in thermal equilibrium during decoupling. However, the resulting transfer function has a very similar shape than the one from thermal decoupling, and there is a direct conversion between the mass of resonantly and thermally produced particles ( $m_{\text{RES}}$  and  $m_{\text{WDM}}$ , respectively), given by the fitting formula  $m_{\text{RES}} \sim 4.43 \text{ keV} (m_{\text{WDM}}/\text{keV})^{4/3}$  from Viel et al. [14]. It is conventional to give the generic thermal mass of the WDM particles  $m_{\text{WDM}}$ , and to estimate the WDM

mass of a specific production mechanism by comparing the transfer functions. In the rest of this letter we will follow this convention.

In the last decade, a number of different authors have proclaimed WDM as a potential solution to observed discrepancies on small scales, however with different WDM particle mass depending on the problem. The excess of dark matter velocity dispersion in the inner parts of Milky-Way satellites, the *too big to fail* problem [15], has been explained by a WDM model with particle mass of  $m_{\text{WDM}} = 1.4 - 2 \text{ keV}$  [16, 17], while the luminosity function from semi-analytical modeling has been shown to be in agreement with a WDM model of  $m_{\text{WDM}} = 0.75$  [18]. The HI velocity function on the other hand seems to be best matched by a WDM with  $m_{\text{WDM}} = 1.0$  [3, 19]. The use of different WDM particle masses depending on the problem leads to the somewhat misleading impression that WDM provides ideal solutions to different regimes of small scale structure formation. However, in order to be consistent, a single particle mass needs to provide a solution to all problems and this specific WDM scenario has to pass all observational constraints.

The major difficulty of using small scale structure formation to constrain the nature of dark matter, is the influence of baryons, which is largely unknown and could produce effects that are degenerate to the expected effects from dark matter [20]. For example, photon evaporation during the epoch of reionization as well as stellar feedback effects from the first stars are expected to blow the gas out of the potential wells of small haloes, to switch off star formation and render them completely dark [21]. Alternatively, stellar feedback could also alter the inner dark matter density profiles of dwarf galaxies, it is however very questionable whether this effect could be large enough to reconcile theory with observations [22].

In this letter, we reconsider the WDM scenario under the light of the latest constraints from Lyman- $\alpha$  forest and SDSS data. Since these constraints exclude most

of the WDM scenarios mentioned above, one should ask the question if the WDM paradigm is still able to alleviate the observed small scale problems. We directly compare circular velocities from the stellar and HI content of observed dwarf galaxies with the velocity dispersions from N-body simulations and analytical models. Since circular velocities trace the underlying dark matter density field, no detailed knowledge of the hydrodynamical interactions is required. The most stringent tests come from the stellar velocities at the half-light radius of dwarf galaxies and from the HI velocities measured with 21cm surveys. We use both of these observations to check whether WDM models within the allowed constraints are still able to solve the small scale crisis present in CDM structure formation.

*WDM particle mass.*— The WDM paradigm has been tested with multiple different observations, leading to independent constraints on the WDM particle mass. Examples are the number of dwarf galaxies [23], weak lensing [24, 25], galaxy formation [26], the Lyman- $\alpha$  forest [27, 28] or gamma ray bursts [29]. Currently, the most stringent constraints come from the Lyman- $\alpha$  forest with  $m_{\text{WDM}} > 3.3$  keV at the  $2\sigma$  level [30]. This measurement is based on the recent comparison of high redshift quasar spectra combined with an extended series of hydrodynamical simulations. Another tight constraint comes from the number of ultra-faint dwarf galaxies in the SDSS data, which sets a bound on the WDM mass of  $m_{\text{WDM}} > 2.3$  ( $2\sigma$ ) with a maximum likelihood of  $m_{\text{WDM}} = 4$  keV [23]. Both constraints rule out WDM models with a mass of  $m_{\text{WDM}} = 1 - 2$  keV, which would be able to resolve some of the CDM small scale problems.

Based on these considerations, we state that a realistic WDM scenario must have a mass of about  $m_{\text{WDM}} \sim 4$  keV to be in perfect agreement with both Lyman- $\alpha$  and SDSS data. In the following, we will test whether such a scenario is able to alleviate the CDM small scale crisis.

*Too big to fail.*— One of the outstanding problems of CDM structure formation is the deep potential wells of the largest Milky Way satellites, leading to circular velocities that are much larger than the observed half-light velocity dispersions of dwarf galaxies. This is called the *too big to fail* problem, referring to the fact that these massive satellites are to “big” in order to “fail” to produce stars due to baryonic feedback effects and hence should be observable. Contrary to the *missing satellite* problem, the *too big to fail* problem is extremely difficult to solve with hydrodynamical feedback effects [22]. However, it could be alleviated, if the subhalo population around the Milky Way lies in the lower few percent of the halo-to-halo variation [31] or if its total mass is considerably smaller than currently expected [31–33], which seems unlikely [34].

Within a WDM scenario of  $m_{\text{WDM}} \sim 2$  keV the *too big to fail* problem naturally disappears because of the considerably shallower profiles of the largest WDM dwarf

galaxies compared to their CDM counterparts. However, it is unclear whether this is still the case for a realistic WDM particle mass of  $m_{\text{WDM}} \sim 4$  keV. In order to test this, we perform nested high resolution N-body simulations centred on a Milky-Way like halo of  $M \sim 1.28 \cdot 10^{12} M_{\odot}$  and analyse the profiles of the largest satellites. For the simulations and the subsequent analysis we use the same setup than in Refs. [17, 35]. The only difference is an improved mass resolution by a factor of 4, corresponding to a simulated particle mass of  $3.4 \cdot 10^4 M_{\odot}$ , and a gravitational softening of 195 pc. The simulations are performed with `pkdgrav`, a parallel tree-code with multiple moment expansion [36] and the halo finding is done with the subhalo finder `6df` [37].

In Fig. 1 we plot the velocity profiles of the 12 satellites with the largest  $V_{\text{max}}$  at infall [see 35, for more information on the method] and compare them to the observed half-light stellar velocity dispersion of 9 classical dwarf galaxies (LMC, SMC and Sagittarius have been removed from the sample). These two measures are directly comparable, since both the dark matter and the stars act as a collisionless fluids in the same potential well. For the CDM case (in the right-hand panel) the profiles (in black) are systematically above the observed dots, showing the standard *too big to fail* discrepancy. In the WDM case with  $m_{\text{WDM}} = 2$  keV (plotted in the left-hand panel) the discrepancy disappears and the profiles (in green) roughly coincide with the observed dots. This WDM scenario seems to solve the *too big to fail* problem, it is however ruled out by the recent constraints from Lyman- $\alpha$  forest and SDSS data (as discussed in the former section). In the case of a realistic WDM scenario with  $m_{\text{WDM}} = 4$  keV (third panel from the left), the circular velocity profiles (in red) are significantly above the values of the observed dwarf galaxies, yielding a similar picture than in the case of CDM. From the content of Fig. 1 it is clear that a realistic WDM scenario that passes the Lyman- $\alpha$  constraints is too cold to significantly alleviate the *too big to fail* problem.

(The grey lines in Fig. 1 are the profiles of all satellites with  $V_{\text{max}} > 12$  km/s, illustrating the *missing satellite* problem. While the amount of satellites in the CDM, the 4 keV and the 3 keV WDM models largely exceeds the observed number of Milky-Way dwarfs, it is roughly comparable in the case of the 2 keV WDM model.)

*HI velocity function.*— Another test of small scale structure formation comes from the HI velocity-width function measured in the local universe by recent 21cm surveys like the Arecibo Legacy Fast ALFA (ALFALFA) survey [38]. The general shape of the HI velocity-width function is characterised by a power-law decrease followed by an exponential drop-off, whereas the slope of the power-law is significantly shallower than the one expected from CDM structure formation. This fact has motivated several authors to consider a shift of the dark matter paradigm and to suggest WDM as a more realistic

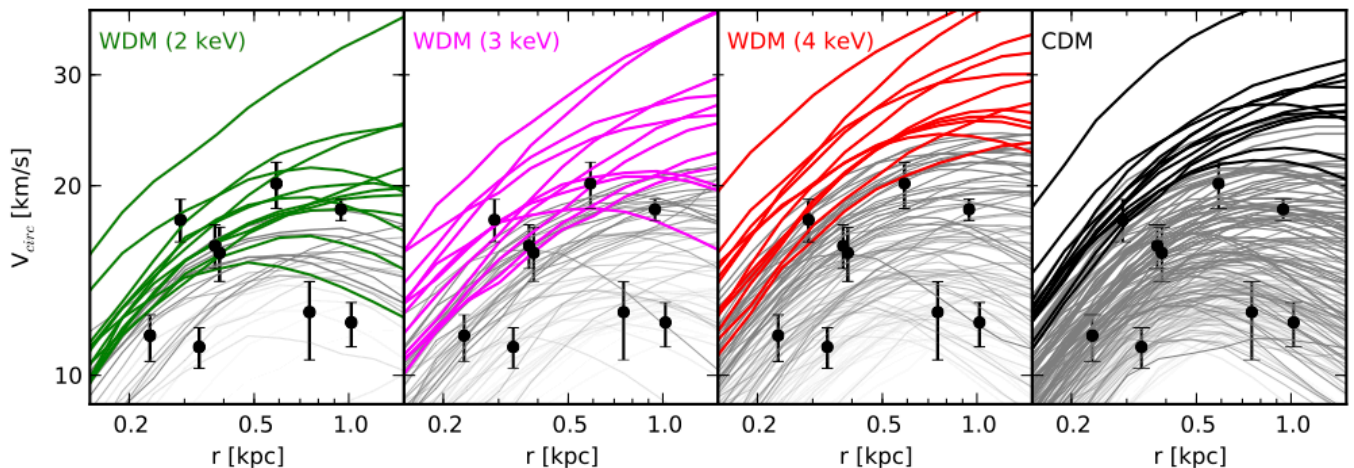


FIG. 1. Circular velocities profiles of the 12 satellites with the highest  $V_{\max}$  at infall (green, magenta, red, and black lines). The observed circular velocity at half-light radius of the 9 classical dwarfs are added as black dots with error-bars (the LMC, SMC and Sagittarius are not displayed). From left to right: WDM with  $m_{\text{WDM}} = 2, 3, 4$ , and CDM. The grey lines are the remaining satellites above  $V_{\max} = 12$  km/s with decreasing line-width for smaller  $V_{\max}$  at infall.

scenario [3, 19]. For example, Zavala et al [3, hereafter Za09] used constrained simulations of the local universe to show that a WDM model with  $m_{\text{WDM}} = 1$  keV leads to a velocity function in much better agreement with observations.

In the following, we revisit this finding in the light of the new constraints of the WDM particle mass, in order to test if a realistic WDM model with  $m_{\text{WDM}} \sim 4$  keV still agrees with observations. Since we are only interested in the general shape of the HI velocity-width function, we will content ourself with simplified analytical descriptions of the HI content in galaxies, without running expensive hydrodynamical simulations. The essential ingredient of our approach is the WDM halo mass function developed in Ref. [39], which is based on the sharp-k window function and works for cosmologies with arbitrary initial power spectra. The functional form is given by

$$\frac{dn}{d \log M} = \frac{\bar{\rho}}{M} f(\nu) \frac{3}{4\pi^2 \sigma^2(R)} \frac{P_{\text{lin}}(1/R)}{R^3}, \quad (1)$$

$$\sigma(R) = \int \frac{dk^3}{(2\pi)^3} P_{\text{lin}}(k) \Theta(1 - kR), \quad (2)$$

where  $\Theta$  is the Heaviside step function and  $f(\nu) = A\sqrt{2\nu/\pi}(1 + \nu^{-p})e^{-\nu/2}$  with  $\nu = (1.686/\sigma)^2$ ,  $A=0.322$ , and  $p=0.3$ . The halo mass is assigned to the filter scale by the relation  $M = 4\pi\bar{\rho}(cR)^3/3$  with  $c = 2.7$ .

From the halo mass function it is possible to construct the HI velocity-width function using some simplified assumptions. The procedure consists in first constructing the maximum circular velocity function (short: velocity function) of haloes and then connecting the circular velocity to the measured velocity-width of the HI disk.

We construct the halo velocity function in the same way as Za09, an approach initially developed by Sigad et al. [40]. The recipe is the following: (i) Producing a mock sample of haloes that mimics the halo mass function for WDM cosmologies (given by Eq. 1). (ii) Assigning an NFW-profile to each halo with a randomly selected concentration out of a log-normal distribution from Ref. [41]. Using the fitting formula of Ref. [8] to adopt the concentration to the WDM scenario. (iii) Calculating the maximum circular velocity ( $V_{\max}$ ) for every mock halo with the help of Eq. 7 in Ref. [40]. (iv) Binning the haloes with respect to their value of  $V_{\max}$  in order to obtain  $dn/d \log V_{\max}$ .

The velocity function of haloes  $dn/d \log V_{\max}$  is plotted in the left-hand-side of Fig. 2, where the blue, green, and red lines represent WDM cosmologies with particle masses of 1, 2, and 4 keV, while the black line represents the standard CDM model. The WDM velocity function has a similar shape than the original halo mass function (plotted in Fig. 5 of Ref. [39]), with a suppression and a downturn below a certain value of  $V_{\max}$ .

The connection between the halo velocity function and the velocity-width function of the HI component consists in setting HI disks into the mock haloes with an appropriate velocity-width  $W_{50}$ . We again closely follow Za09, utilizing the following recipe: (i) Populating every mock halo below  $10^{13} M_{\odot}/h$  with exactly one HI disk [42]. (ii) Calculating the maximum circular velocity of the disk ( $V_{\max,d}$ ) with the help of Eq. (1) from Za09, using a disk-to-halo mass ratio  $f = 0.03$  and a halo spin  $\lambda = 0.032$ . This leads to the approximative relation  $V_{\max,d} \sim 1.18V_{\max}$ . (iii) Connecting the velocity-width to the disk circular velocity by setting  $W_{50} = 2V_{\max,d}$ . (iv) Changing the density criterion by a factor of three

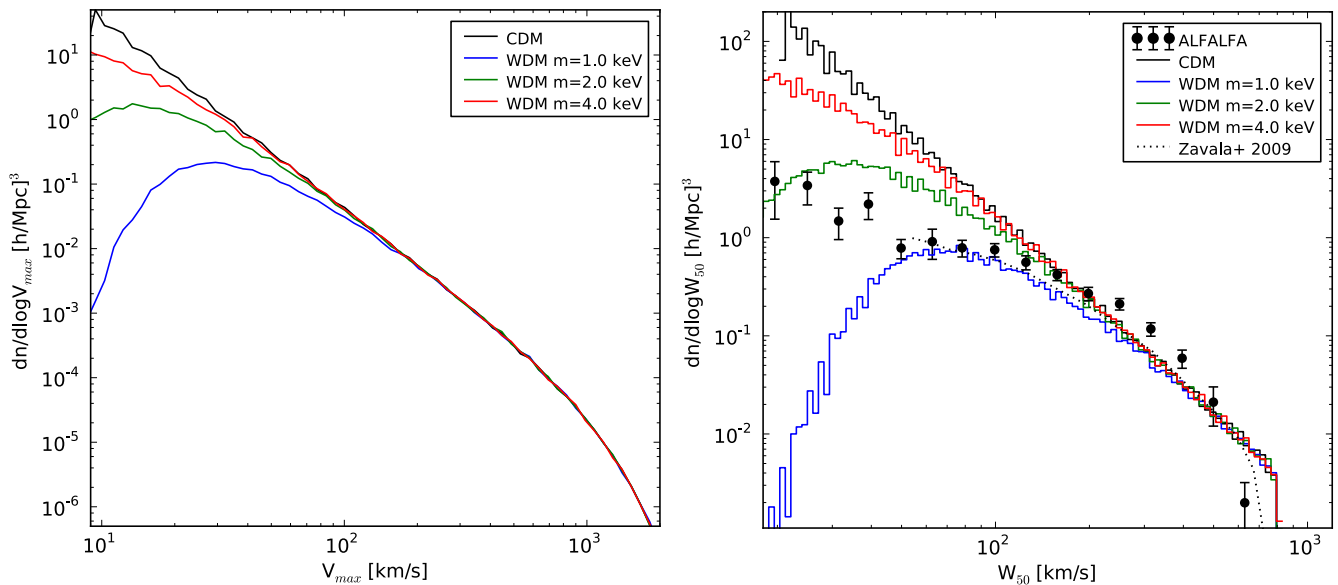


FIG. 2. *Left panel:* Maximum circular velocity function of haloes constructed with the massfct of Eq. (1) and with assigned random concentrations from a log-normal distribution. Black: CDM; red: WDM, 4keV; green: WDM, 2keV; blue: WDM 1keV. *Right panel:* Velocity-width function of the HI component measured by ALFALFA (black dots) and obtained by converting  $V_{max}$  into  $W_{50}$  as explained in the text. Same colour coding. The simulated velocity-width function from Zavala et al [3] is given as a black dotted line for comparison.

to take into account overdensity of the local universe observed by ALFALFA. (v) Binning the disks with respect to their value of  $W_{50}$  to obtain  $dn/d\log W_{50}$ .

The velocity-width function  $dn/d\log W_{50}$  is plotted in the right-hand-side panel of Fig. 2, where the blue, green, and red lines represent WDM models with 1, 2 and 4 keV, while the black line represents the CDM cosmology. The observed data from the ALFALFA surveys is plotted as black dots. The faint dotted line is the result from Za09, which is based on constrained simulations of the local universe with a 1 keV WDM model and has a resolution limit of  $W_{50} = 36$  km/s. It shows good agreement with both the ALFALFA observations and with our analytical approach (blue line). Below the resolution limit of this simulation, our analytical model starts to decrease and significantly underestimates the amount of observed structures. This shows that the WDM model with  $m_{WDM} = 1$  keV is too extreme to describe the ALFALFA observation, something that was not visible in earlier studies because of limited resolution. A WDM model with a realistic particle mass of 4 keV, on the other hand, shows only a small suppression with respect to the CDM model, which is by far not sufficient to explain the observations. This shows that a realistic WDM model, which passes all constraints from the Lyman- $\alpha$  forest and SDSS data, is not able to explain the apparent flatness of the HI velocity-width function.

*Conclusions.*— We have tested the WDM paradigm on two of the most prominent small scale problems of CDM structure formation, the *too big to fail* problem of the

largest Milky Way satellites and the *flatness* problem of the HI velocity-width function in the local universe. As a result, we show that a realistic WDM scenario with  $m_{WDM} = 4$  keV in agreement with recent constraints from Lyman- $\alpha$  forest and SDSS data is not able to alleviate the the small scale crisis of CDM structure formation. The reason for this failure is the cutoff in the linear power spectrum, which is too steep to simultaneously agree with both constraints from the Lyman- $\alpha$  forest and from observations of ultra-faint dwarf galaxies.

The shape of the linear power spectrum is sensitive to the details of the dark matter production mechanism, and thermal production as well as the standard sterile neutrino production based on oscillations lead to a very steep drop-off that is impossible to reconcile with all observations. From an astrophysical point of view, these production mechanisms are therefore disfavored, in the sense that they do not show better agreement with dwarf galaxy observations than the standard CDM picture of weakly interacting massive particles (WIMPs).

A potentially promising way out are alternative sterile neutrino production mechanisms based on a mixture of non-resonantly produced warm and resonantly produced cold particles, leading to mixed dark matter (MDM) scenario with a step in the power spectrum instead of a cut-off [43, 44]. Recent studies on the structure formation of such models are promising [17, 35, 45], but more investigation is necessary to test whether these alternative approaches agree with both Lyman- $\alpha$  forest and ultra faint dwarf galaxies.

We thank Darren Reed for important inputs on the construction of velocity functions and William Watson for providing the title of the paper. AS acknowledges support from the European Commissions Framework Programme 7, through the Marie Curie Initial Training Network CosmoComp (PITNGA-2009-238356). All simulations have been performed on the SuperMuc and Theo clusters in Munich and the zbox4 cluster in Zurich.

\*aurel.schneider@sussex.ac.uk

- 
- [1] Klypin, A., Kravtsov, A. V., Valenzuela, O., Prada, F. 1999, *ApJ*, 522, 82
- [2] Moore, B., Ghigna, S., Governato, F., Lake, G., Quinn, T., Stadel, J., Tozzi, P. 1999, *ApJ*, 524L, 19M
- [3] Zavala, J., Jing, Y. P., Faltenbacher, A., Yepes, G., Hoffman, Y., Gottlöber, S., Catinella B. 2009, *ApJ*, 700, 1779
- [4] Tikhonov, A. V., Klypin, A. 2009, *MNRAS*, 395, 1915
- [5] de Blok, W. J. G. McGaugh, S. S., Bosma, A., Rubin, V. C. 2001, *ApJ*, 552, 23
- [6] Weinberg, D., Bullock, J., Governato, F., Kuzio de Naray, R., Peter, A. H. G. 2013, arXiv:1306.0913
- [7] Bode, P., Ostriker, J. P., & Turok, N. 2001, *ApJ*, 556, 93
- [8] Schneider, A., Smith, R. E., Macciò, A. V., Moore, B. 2012, *MNRAS*, 424, 684S
- [9] Macciò, A. V., Paduroiu, S., Anderhalden, D., Schneider, A., & Moore, B. 2012, *MNRAS*, 424, 1105M
- [10] de Vega, H. J., Salucci, P., & Sanchez, N. G. 2013, arXiv:1309.2290
- [11] Gonzalez-Garcia, M. C., Maltoni, M. 2008, *Phys. Rev.* 460, 1
- [12] Dodelson, S., Widrow, L. M. 1994, *Phys. Rev. L.* 72, 17
- [13] Shi, X., Fuller, G. M. 1999, *Phys. Rev. L.* 82, 2832
- [14] Viel, M., Lesgourgues, J., Haehnelt, M. G., Matarrese, S., & Riotto, A. 2005, *Phys. Rev. D*, 71, 063534
- [15] Boylan-Kolchin, M., Bullock, J. S., Kaplinghat, M., 2012, *MNRAS*, 422, 1203
- [16] Lovell, M., Eke, V., Frenk, C., Gao, L., Jenkins, A., Theuns, T., Wang, J., Boyarsky, A., & Ruchayskiy, O. 2012, *MNRAS*, 420, 2318L
- [17] Anderhalden, D., Diemand, J., Bertone, G., Macciò, A. V., & Schneider A. 2012, *JCAP*, 10 047A
- [18] Menci, N., Fiore, F., Lamastra, A., 2013, *MNRAS*, 766, 110
- [19] Papastergis, E., Martin, A. M., Giovanelli, R., Haynes, M. P. 2011, *ApJ*
- [20] Herpich, E., Stinson, A. M., Macciò, A. V., Brook, C., Wadsley, J., Couchman, H. M. P. Quinn, T. 2013, arXiv:1308.1088
- [21] Macciò, A. V., Kang, X., Fontanot F., Somerville, R S., Kopolov, S., Monaco, P. 2010, *MNRAS*, 402, 1995M
- [22] Garrison-Kimmel, S., Rocha, M., Boylan-Kolchin, M., Bullock, J. S., Lally, J. 2013, *MNRAS*, 433, 3539G
- [23] Polisensky, E. & Ricotti, M. 2010, *Phys. Rev D*, 83, 043506
- [24] Miranda M., Macciò, A. V. 2007, *MNRAS*, 382, 1225M
- [25] Smith, R. E. & Markovic, K. 2011, *Phys. Rev. D*, 84, 063507
- [26] Macciò, A. V. & Fontanot, F. 2010, *MNRAS*, 404, L16
- [27] Seljak, U, Makarov, A., McDonald, P., Trac, H. 2006, *Phys. Rev. Lett.*, 97, 191303
- [28] Viel, M., Lesgourgues, J., Haehnelt, M. G., Matarrese, S., Riotto, A. 2006, *Phys. Rev. Lett.*, 97, 071301
- [29] de Souza, R. S., Mesinger, A., Ferrara, A., Haiman, Z., Perna, R., Yoshida, N. 2013, arXiv:1303.5060
- [30] Viel, M., Becker, G. D., Bolton, J. S., Haehnelt, M. G., A. 2013 arXiv e-print
- [31] Purcell, C. W., & Zentner, A. R. 2012, *JCAP*, 12, 7
- [32] Wang, J., Frenk, C. S., Navarro, J. F., Gao, L., & Sawala, T. 2012, *MNRAS*, 424, 2715
- [33] Rashkov, V., Madau, P., Kuhlen, M., & Diemand, J. 2012, *ApJ*, 745, 142
- [34] Boylan-Kolchin, M., Bullock, J. S., Sohn, S. T., Besla, G., & van der Marel, R. P. 2013, *ApJ*, 768, 140
- [35] Anderhalden, D., Schneider A., Macciò, A. V., Diemand, J., & Bertone, G. 2013, *JCAP*
- [36] Stadel, J. G. 2001, Thesis (PhD), University of Washington.
- [37] Diemand, J., Kuhlen, M., & Madau, P. 2006, *ApJ*, 649, 1
- [38] Giovanelli, R., et al. 2005, *AJ*, 130, 2613
- [39] Schneider, A., Smith, R. E., Reed, D. 2013, *MNRAS*, 433, 1573S
- [40] Sigad, Y., Kolatt, T. S., Bullock, J. S., Kravtsov, A. V., Klypin, A. A., Primack, J. R., Deckel, A. 2000, arXiv:astro-ph/0005323
- [41] Macciò, A. V., Dutton, A. A., van den Bosch, F. C 2008, *MNRAS*, 391, 1940
- [42] This is motivated by the fact that satellite galaxies have lost their gas due to dynamical friction (see Za09 for a detailed discussion on the validity of this approximation)
- [43] Boyarsky A., Ruchayskiy O., & Shaposhnikov, M. 2009, *Annual Review of Nuclear and Particle Science*, 59, 191
- [44] Boyarsky, A., Lesgourgues, J., Ruchayskiy, O., & Viel, M. 2009, *JCAP*, 5, 12
- [45] Macciò, A. V., Ruchayskiy, O., Boyarsky, A., & Muñoz-Cuartas, J. C. 2012, *MNRAS*, 428, 882M